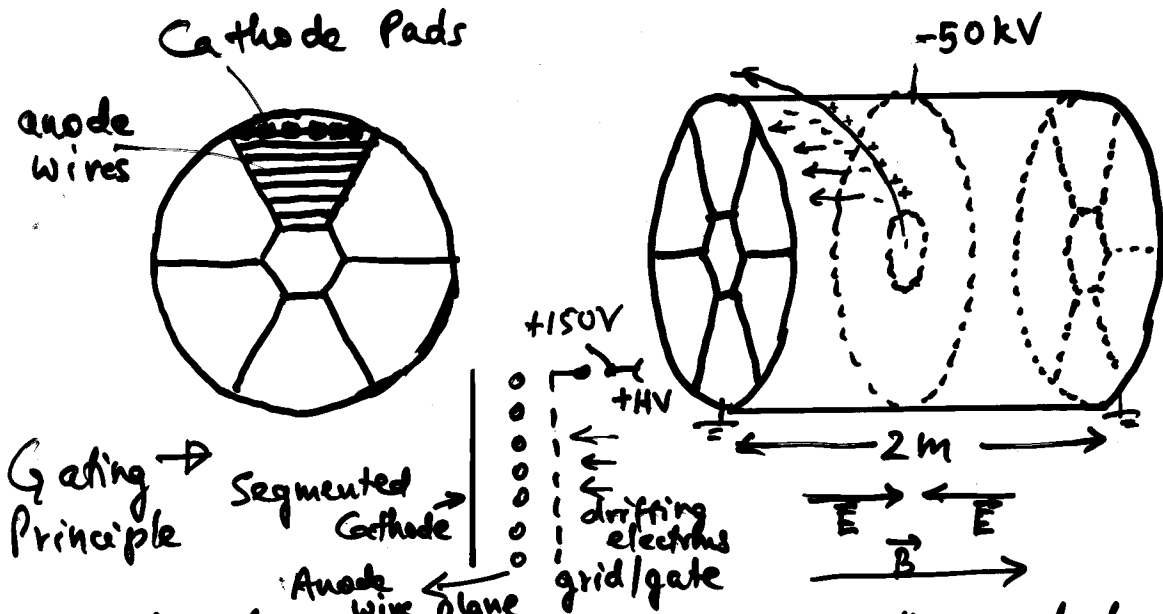


Time Projection Chamber

- Full 3D track reconstruction
- Optimal tracking as far as minimizing multiple scattering & photon conversions are concerned.



- Apart from counting gas, the detector contains no other constructional elements
- Huge drift volume
- Typical counting gas Ar/CH₄ (90%/10%)
- Chamber divided into 2 halves by means of a central electrode.

End plates with MWPC configuration

- Z-coordinate measured by drift time
- γ by anode wires and ϕ by cathode pads
- Diffusion significantly reduced by B-field.
- Space-charge problem avoided by gating

Drift Chambers

Time Projection Chamber → full 3-D track reconstruction

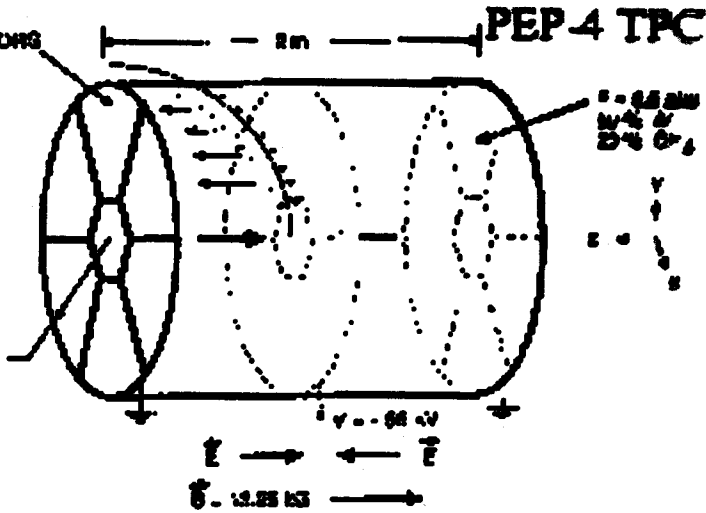
- ◆ x-y from wires and segmented cathode of MWPC
- ◆ z from drift time
- ◆ in addition dE/dx information

Diffusion significantly reduced by B-field.

Requires precise knowledge of $v_p \rightarrow$
LASER calibration +
 p, T corrections

Drift over long distances → very good gas quality required

Space charge problem from positive ions, drifting back to midwall → gating

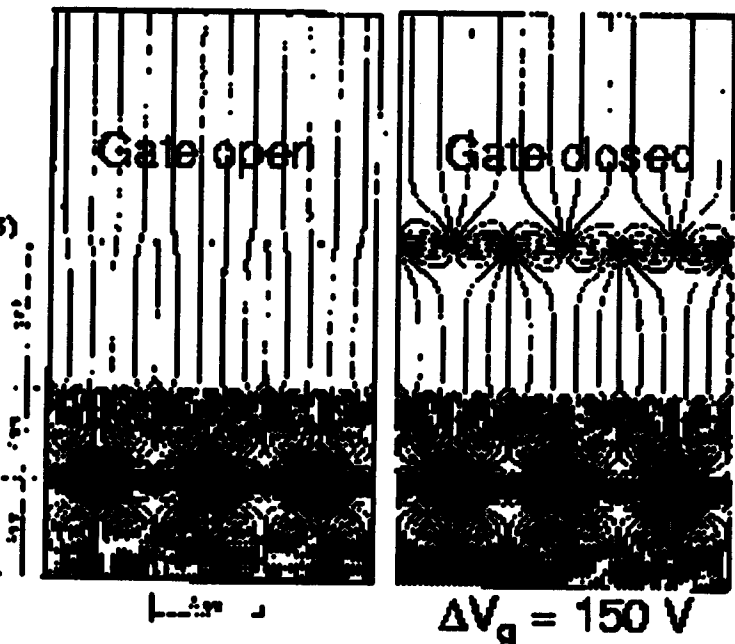


ALEPH TPC

(ALEPH coll., NIM A 294 (1990) 121,
W. Atwood et. al, NIM A 305 (1991) 445)

Ø 3.6M, L=4.4 m

$\sigma_{R\phi} = 173 \mu\text{m}$
 $\sigma_z = 740 \mu\text{m}$
 (isolated leptons)



~~Pus kya Bh~~

10/27/20

CALORIMETRY

- Extremely versatile detectors
- Main application is measurement of energy of electrons, photons and hadrons by total absorption (hence "destructive" method)
 - Detector response $\propto E$
 - Size of the calorimeter scales as $\ln E$ and performance improves with energy (tracking volume scales like \sqrt{E})
- A variety of other measurements possible: position, angle; particle ID, triggering
- Works for both charged (e , hadrons) and neutral particles (n, γ)
- Basic mechanisms:
electromagnetic and strong interactions producing showers of secondary particles with progressively degraded energy
- Basic Types:
 - Electromagnetic and Hadronic Calorimeters
 - Sampling and Homogeneous Calorimeters.

Electromagnetic calorimeters:

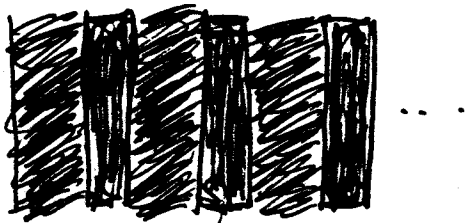
used mainly to measure/detect electrons and photons through their electromagnetic interactions (e.g., Bremsstrahlung, Pair Production)

Hadronic calorimeters:

Used to measure mainly hadrons through their strong and electromagnetic interactions.

Sampling Calorimeters:

Consist of alternating layers of an absorber, a dense material to degrade energy (induce showering) and an active medium to detect the signal



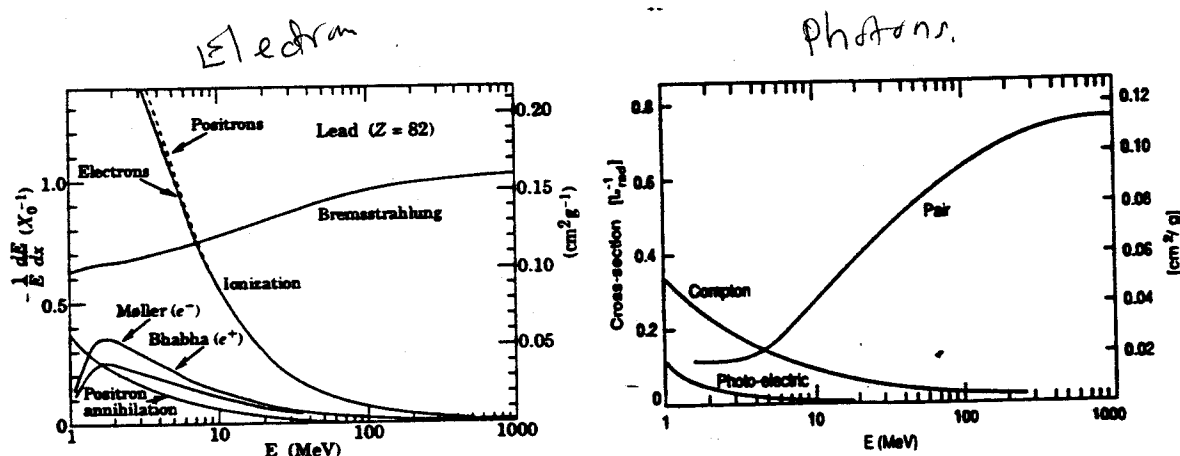
/
Could be gaseous, liquid or solid medium for detection

Homogeneous Calorimeters:

Built of one type of material which performs both tasks, energy degradation and signal generation

PHYSICS OF ELECTROMAGNETIC SHOWERS

- For $E \gtrsim 10 \text{ MeV}$, the dominant energy loss mechanism for electrons is Bremsstrahlung and for photons, it is Pair production.
- For $E > 1 \text{ GeV}$, both processes become essentially energy independent.



For $E < 10 \text{ MeV}$, electrons lose their energy through ionization, mainly; photons lose energy through Compton Scattering and photoelectric effect.

The energy at which Ionization loss \equiv Brem loss

$$\Rightarrow E_c \sim \frac{800 \text{ MeV}}{Z} \quad (\text{Critical Energy})$$

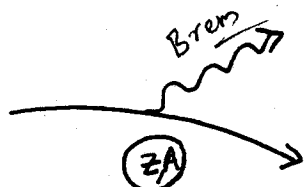
$$\left. \frac{dE}{dx} (E_c) \right|_{\text{ion}} = \left. \frac{dE}{dx} (E_c) \right|_{\text{Brem}}$$

Energy Loss of electrons by Bremsstrahlung:

$$-\frac{dE}{dx} = \frac{E}{X_0}$$

Radiation length

$$\text{where } X_0 \approx \frac{A}{4\alpha N_A Z^2 r_e^2 \ln \frac{183}{Z^{1/3}}} \approx \frac{180 A}{Z^2} \text{ g/cm}^2$$



(remember X_0 is defined for electrons, and $X_0 \propto m^2$)

$$E(x) = E_0 e^{-x/X_0}$$

$$\begin{aligned} X_0(\text{H}_2) &= 8.65 \text{ cm} \\ \text{Al} &: 8.9 \text{ cm} \\ \text{Pb} &: 5.6 \text{ mm} \\ \text{U} &: 3.2 \text{ mm} \end{aligned}$$

i.e., X_0 is the average distance that an electron must travel in a material to reduce its energy to $\frac{1}{e}$ of the original energy.

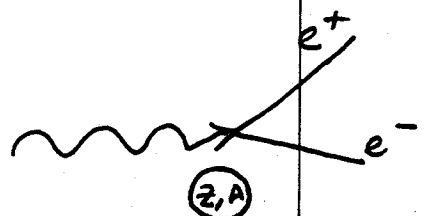
Pair (e^+e^-) production for photons:

$$\Gamma_{\text{pair}} = 4\alpha r_e^2 Z^2 \left[\frac{7}{9} \ln \frac{183}{Z^{1/3}} \right]$$

$$\approx \frac{7}{9} \frac{A}{N_A} \cdot \frac{1}{X_0}$$

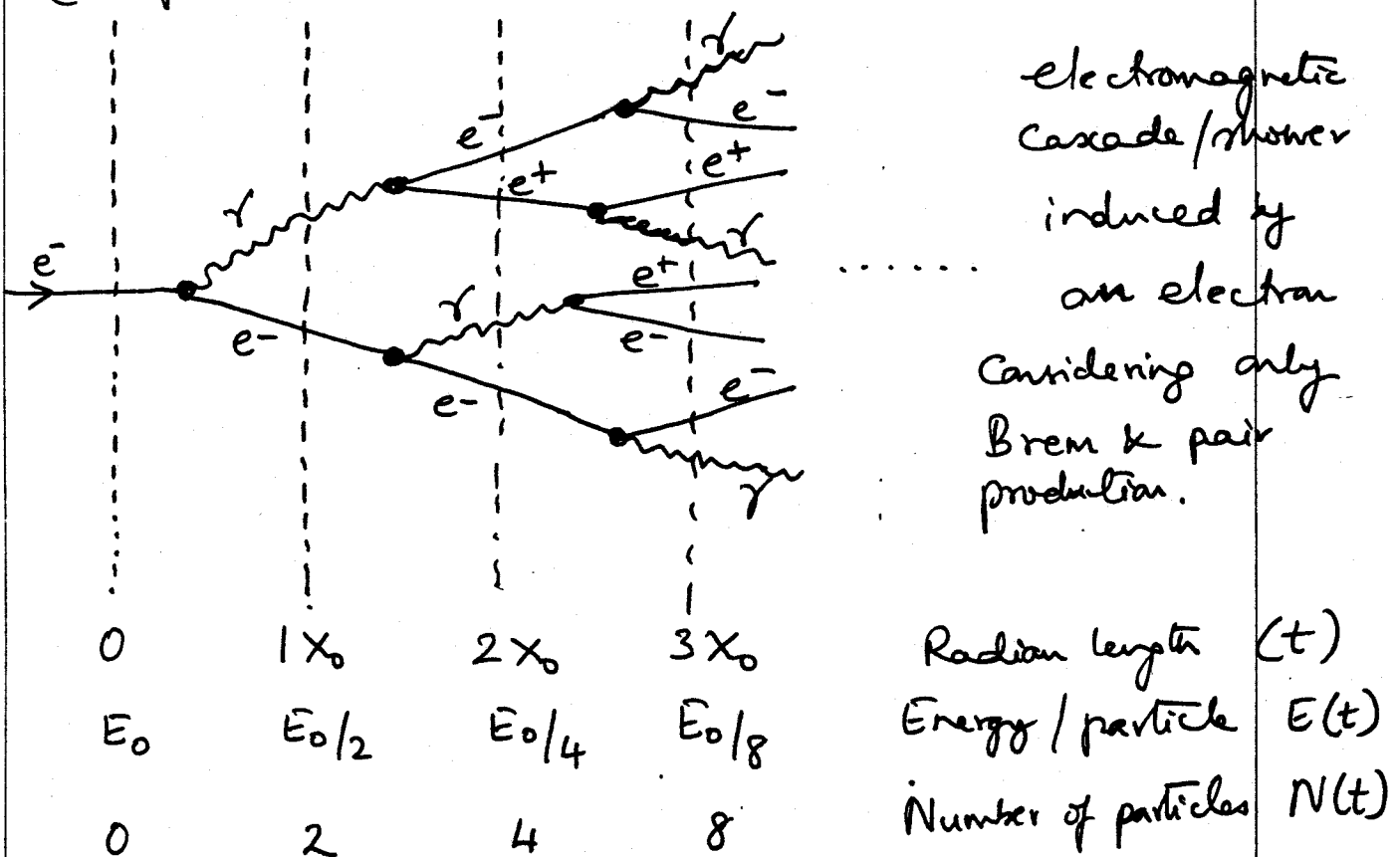
$$\therefore \lambda_{\text{pair}} = \frac{9}{7} X_0$$

$$I(x) = I_0 e^{-\frac{7}{9} \frac{x}{X_0}}$$



The intensity of photons is reduced by $\frac{1}{e}$ of original intensity after a distance $\frac{9}{7} X_0$

- The physical scale over which the showers develop are similar for incident electrons and photons.
- ∴ The electromagnetic showers are described in a universal way using simple functions of X_0 .
(Simple model due to Heitler (1953))



After t radiation lengths,

$$N(t) = 2^t = e^{t \ln 2}$$

$$E(t) = E_0 / 2^t$$

Cascade continues to develop as long as $E(t) > E_c$

The depth at which the shower energy equals some value E' occurs when $E(t) = E'$

Average energy at depth "t",
i.e., $E' = E_0 / 2^{t(E')}$ = $\frac{E_0}{e^{t(E') \ln 2}}$

$$\frac{E_0}{E'} = e^{t(E') \ln 2}$$

$$\therefore t(E') = \frac{\ln(E_0/E')}{\ln 2}$$

Since the production of particles stops at $E(t) = E_c$, the shower has maximum number of particles when $E(t) = E_c$.

So, the "shower-max" depth is,

$$t_{\max} = \frac{\ln(E_0/E_c)}{\ln 2}$$

\leftarrow indicating the detector thickness needed to absorb a shower

Note: Maximum shower depth increases logarithmically with primary energy

Number of particles at shower-max is,

$$N_{\max} = e^{t_{\max} \ln 2} = \frac{E_0}{E_c}$$

\therefore The number of particles at shower max $\propto E_0$!

The number of particles in the shower with $E > E'$ ($E' \ll E_0$) would be,

$$N(E > E') = \int_0^{t(E')} N(t) dt$$

$$= \int_0^{t(E')} e^{t \ln 2} dt \approx \frac{1}{\ln 2} \cdot \frac{E_0}{E'}$$

$$\therefore \frac{dN}{dE'} \propto \frac{1}{E'^2}$$

The sum of all charged track lengths in the shower,

$$L = \frac{2}{3} \int_0^{t_{\max}} N(t) dt \approx \frac{E_0}{E_c}$$

$$\frac{1}{3} \gamma', \frac{1}{3} e^+, \frac{1}{3} e^-$$

- \therefore The total charged track length $\propto E_0$
- \Rightarrow total ionization in the material $\propto E_0$
- \therefore we can measure the energy of the incident particle by measuring ionization produced by the shower particles.

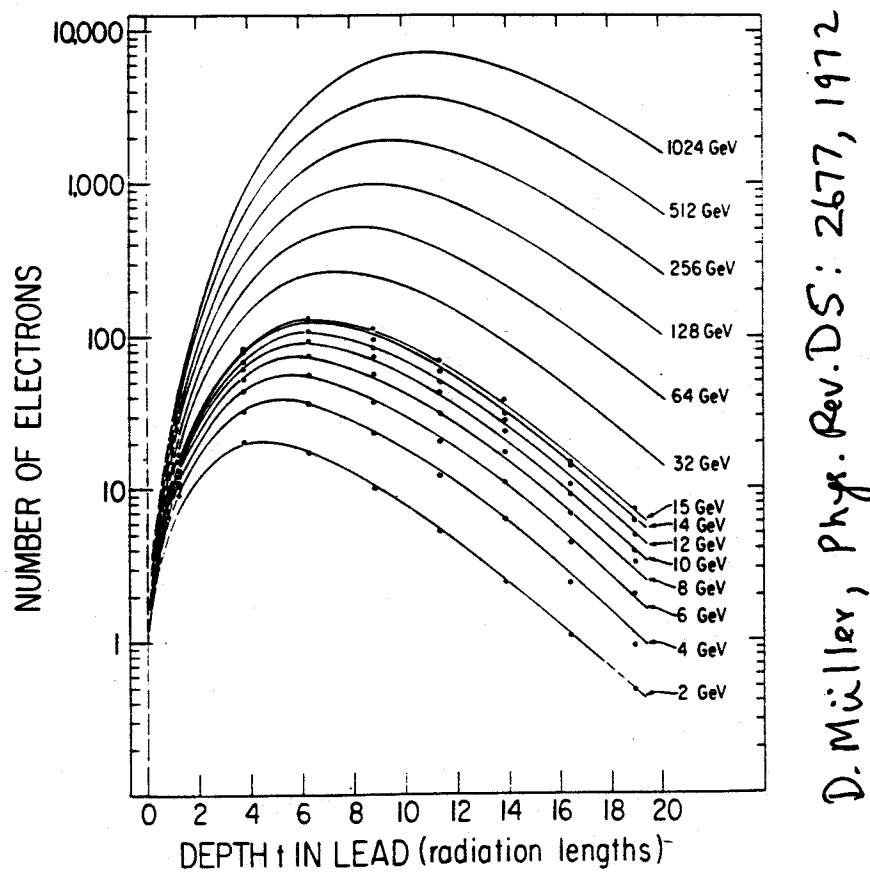
Heitler's assumptions: "This is a simple model"

1. An electron with $E > E_c$ travels $1 x_0$ and then gives up half its energy to a brems photon.
2. A photon with $E > E_c$ travels $1 x_0$ and undergoes pair production with each created particle receiving half of the energy of the photon.
3. Electrons with $E < E_c$ cease to radiate and lose their energy and lose their remaining energy to collisions.
4. Photons with $E < E_c$ cease to pair-produce and interact via Compton effect and photoelectric effect, etc.
5. Neglect ionization and other mechanisms of energy loss for $E > E_c$.

In the simple model considered, the shower abruptly stops at t_{\max} . This discontinuous behaviour is due to the oversimplified assumptions.

More accurate treatments of shower development should take into account the energy dependence of the cross section, the lateral spread of the shower due to multiple scattering, etc.

→ Discontinuity at t_{\max} is broadened into a long tail.



Longitudinal Shower Development:

$$\frac{dE}{dt} \propto t^\alpha e^{-t}$$

$$t_{\max} = \ln \frac{E_0}{E_c} \cdot \frac{1}{\ln 2}$$

$$t_{95\%} \approx t_{\max} + 0.08Z + 9.6 \quad (95\% \text{ containment depth})$$

E.g.: For 100 GeV e^- in Uranium:

$$E_c = 8.7 \text{ MeV}, t_{\max} \sim 13 X_0 \quad t_{95\%} \approx 30 X_0 \\ = 9.6 \text{ cm}$$

DØ calorimeters have EM sections with depth $\sim 20 X_0$, backed up by $\gamma - 10 \cancel{\gamma} \lambda_a$ (interaction lengths)

Transverse Shower Development:

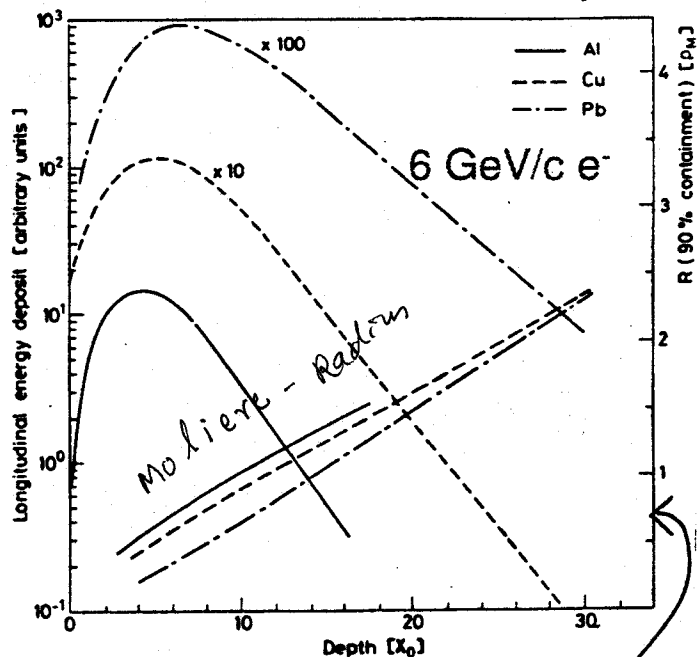
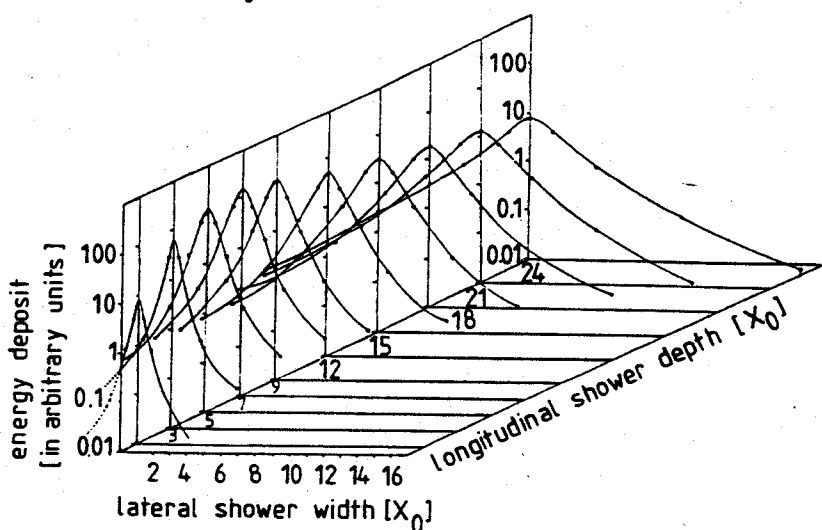
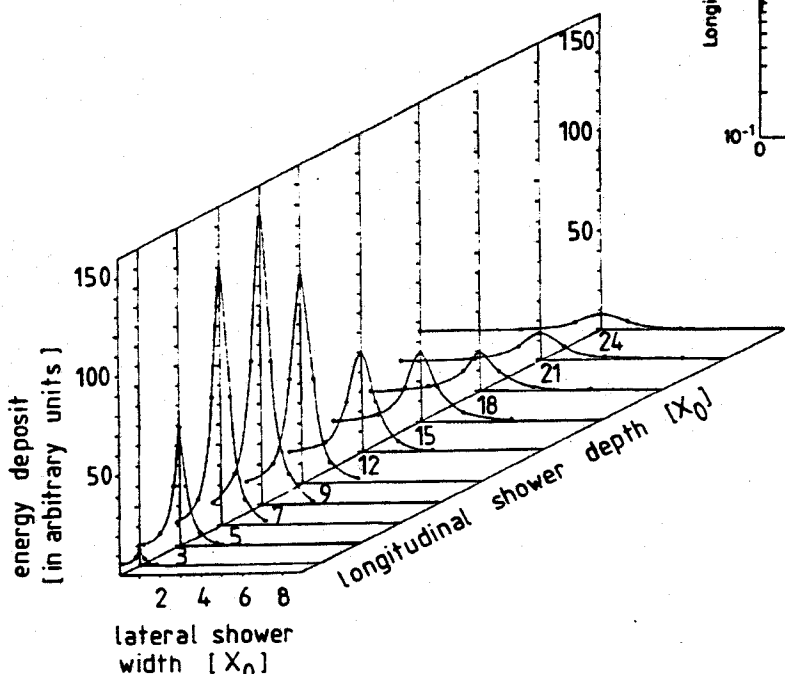
Shower spreads laterally as it penetrates deeper into the material.

95% of the shower cone is located in a cylinder with radius $2R_m$ (R_m = Moliere Radius)

$$R_m = \frac{21 \text{ MeV}}{E_c} \cdot X_0 \quad (\text{g/cm}^2)$$

$$\text{e.g., Uranium: } R_m = 2.4 X_0 \approx 0.77 \text{ cm}$$

Longitudinal shower development in different materials



90% lateral shower containment

Fig. 7.23. Longitudinal and lateral development of an electron shower (6 GeV) in lead shown with linear and logarithmic scales (based on [504, 505]).

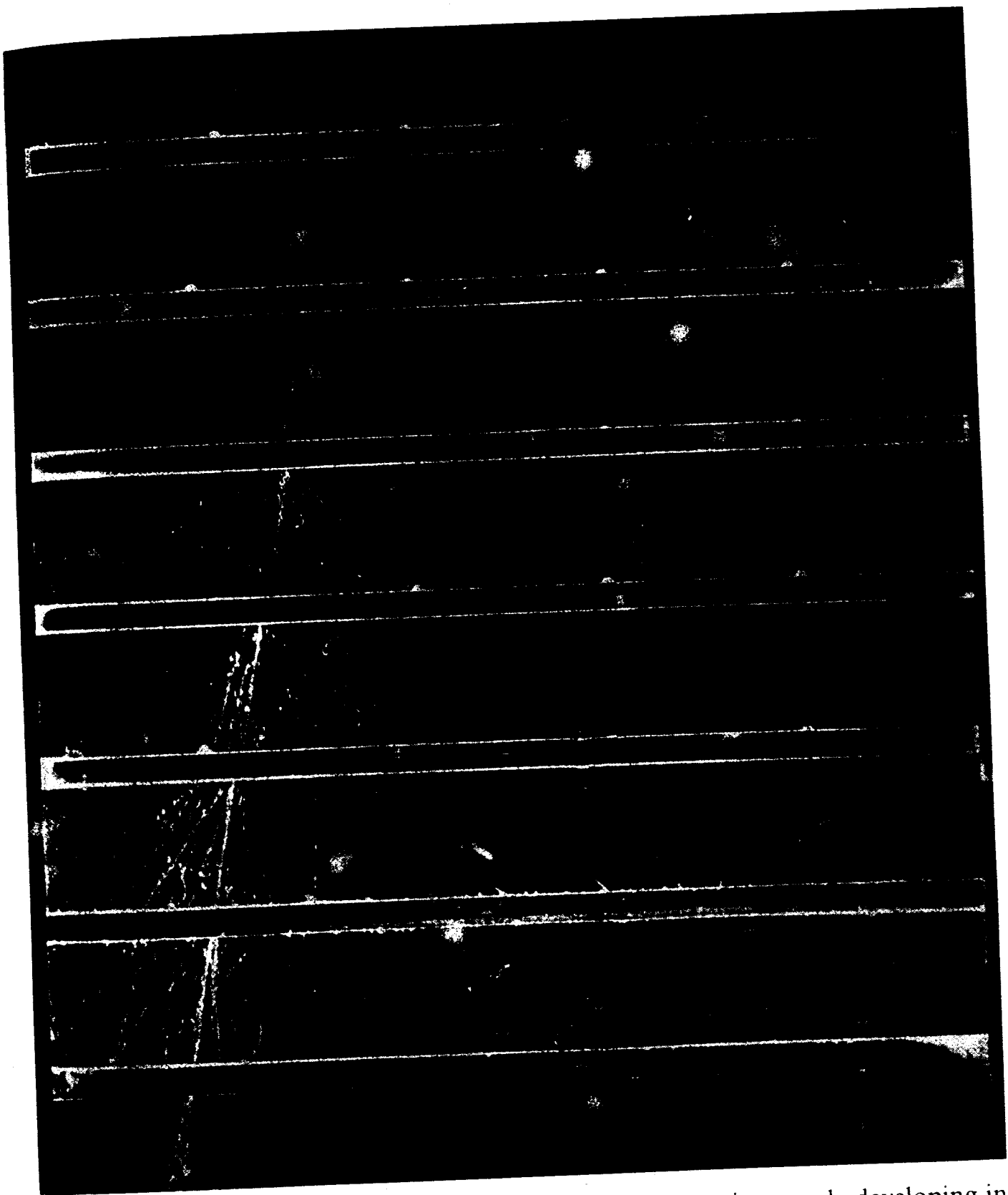


Fig. 11.1. Cloud chamber photograph of an electromagnetic cascade developing in spaced lead plates. (From Ref. 11.11, with permission.)

Energy Resolution :

$$N_{\text{total}} \propto \frac{E_0}{E_c}$$

Total charged particle track length

$$T \propto \frac{E_0}{E_c} ; \text{ Measured ionization} \propto T \propto \frac{E_0}{E_c}$$

$$T_{\text{det}} = F(\xi) T \quad \xi \propto \frac{E_{\text{cut}}}{E_c}$$

↑
detectable track length above energy E_{cut}

$$\frac{\sigma(E)}{E} \propto \frac{\sigma(T_{\text{det}})}{T_{\text{det}}} \propto \frac{1}{\sqrt{T_{\text{det}}}} \propto \frac{1}{\sqrt{E_0}}$$

More generally, if we expand the variance into a power series in E

$$\sigma^2(E) = \sigma_0^2 + \sigma_1^2 E + \sigma_2^2 E^2 + \dots$$

$$\left(\frac{\sigma(E)}{E} \right)^2 = \frac{\sigma_0^2}{E^2} + \frac{\sigma_1^2}{E} + \frac{\sigma_2^2}{E^2} + \dots$$

$$\alpha \quad \boxed{\frac{\sigma(E)}{E} = \frac{a}{\sqrt{E}} \oplus \frac{b}{E} \oplus c}$$

Dominant term in most
calorimeters.

$$\frac{\sigma(E)}{E} = \frac{a}{\sqrt{E}} + \frac{b}{E} + c$$

Stochastic term

Intrinsic fluctuations
in the shower
development

Noise term

Electronic noise
radioactivity
pile-up

Constant term
All contributions
that do not
depend on energy

T_{from}
Imperfection.
Calibration etc.
non-linearity.

Stochastic Term: (Sampling Term)

In homogeneous calorimeters, intrinsic fluctuations are very small.

- energy deposited in the active volume of the detector by a monochromatic beam of particles does not fluctuate event by event
- the resolution better by "Fano Factor"
- a few %

There are not
tributaries
than that and
therefore
resolution
is not better

In Sampling calorimeters, there are variations in the number of charged particles that cross the active layers.

$$N_{\text{ch}} \sim \frac{E_0}{t}; \quad t = \text{thickness of absorber layers in } X_0.$$

$$\therefore \frac{\sigma(E)}{E} \sim \frac{1}{\sqrt{N_{\text{ch}}}} \sim \sqrt{\frac{t}{E_0(\text{GeV})}}$$

\Rightarrow smaller resolution with smaller t or more sampling.

Noise Term:

- Electronic Noise
 - depends on detection technique and read-out electronics
 - Scintillator-based sampling & homogeneous calorimeters have small levels of noise.
 - charge collection techniques yield higher noise
- increases with decreasing energy
Keep noise $< 100 \text{ MeV/channel}$
- noise term reduced by increasing sampling fraction, due to increased signal amplitude
- Radioactivity
- "Pile-up" due to several events in one crossing are adjacent crossing

Constant term:

- Variation of the calorimeter response as a function of shower position arising due to non-uniformities
 - mechanical imperfections
 - or non-uniformity in read-out systems
 - temperature gradients
 - detector aging
 - radiation damage
- Calibration uncertainties
(variation in cell-to-cell calibrations)

PHYSICS OF HADRONIC SHOWERS

- Hadrons produce a cascade of secondary particles: charged and neutral pions, neutrons, protons, etc.
 $\langle N \rangle \propto \ln E$; $\langle p_T \rangle \sim 0.35 \text{ GeV/c}$.
- More complex than electromagnetic showers because of the nature of strong interactions and because they are made up of both hadronic and electromagnetic components.
 - π^0 's $\rightarrow 2\gamma \rightarrow$ electromagnetic cascade
- For $E > 1 \text{ GeV}$, the cross-sections depend only weakly on the energy and on the type of the incident particle
- In analogy to λ_0 , we can define a hadronic absorption length,

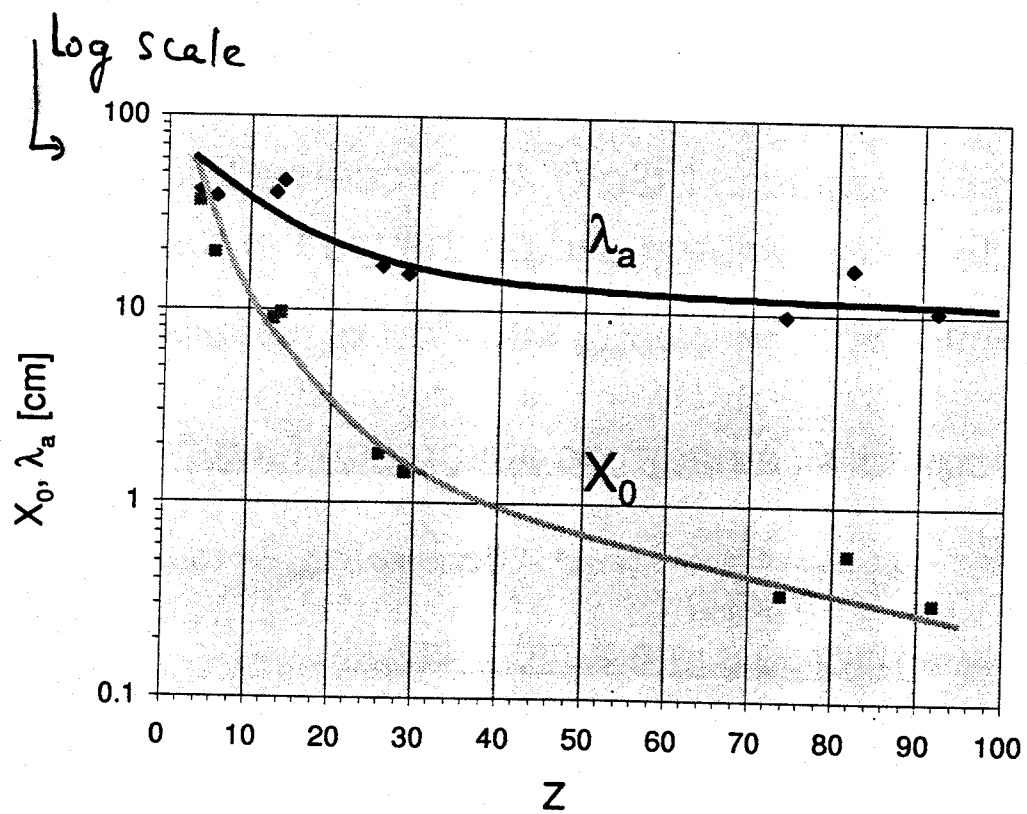
$$\lambda_a = \frac{A}{N_{\text{eff}} \cdot \sigma_{\text{inel}}} \quad \sigma_0 \approx 35 \text{ mb}$$

and a hadronic interaction length

$$\lambda_I = \frac{A}{N_{\text{eff}} \cdot \sigma_{\text{tot}}} ; \quad \lambda_I < \lambda_a$$

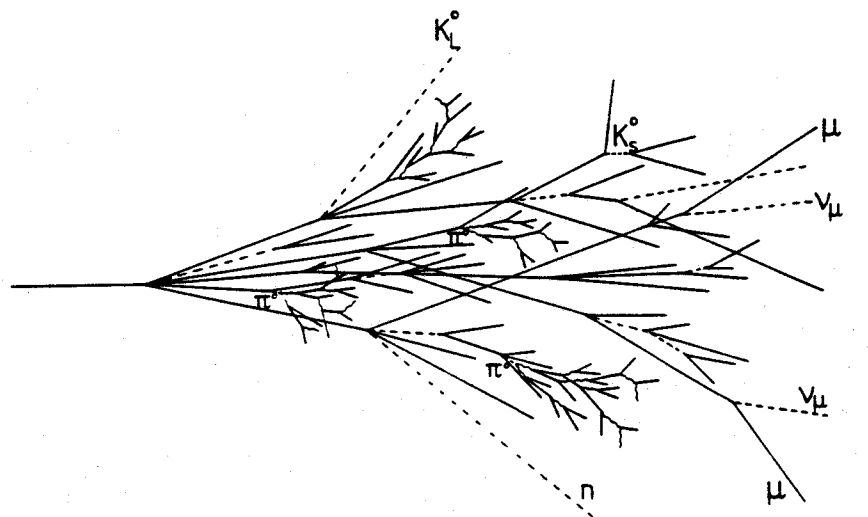
Material	Z	A	ρ [g/cm ³]	X_0 [g/cm ²]	λ_a [g/cm ²]	λ_a [cm]
Hydrogen (gas)	1	1.01	0.0899 (g/l)	63	50.8	
Helium (gas)	2	4.00	0.1786 (g/l)	94	65.1	
Beryllium	4	9.01	1.848	65.19	75.2	
Carbon	6	12.01	2.265	43	86.3	
Nitrogen (gas)	7	14.01	1.25 (g/l)	38	87.8	
Oxygen (gas)	8	16.00	1.428 (g/l)	34	91.0	
Aluminium	13	26.98	2.7	24	8.9	106.4
Silicon	14	28.09	2.33	22		106.0
Iron	26	55.85	7.87	13.9	1.8	131.9
Copper	29	63.55	8.96	12.9		134.9
Tungsten	74	183.85	19.3	6.8		185.0
Lead	82	207.19	11.35	6.4		194.0
Uranium	92	238.03	18.95	6.0	0.31	199.0

For $Z > 6$: $\lambda_a > X_0$ $\lambda_a \sim 35 \cdot A^{1/3} g/cm^2$



- Lots of secondary particles produced in each interaction. Transverse energy of secondaries considerable so, shower spreads out more transversely than e.m. shower.

Average charge multiplicity
 $\bar{c} \gamma =$



- λ , the mean-free path between interactions large $\sim 10\text{ cm}$ in U , 17 cm in Fe .

Max of hadronic shower

$$t_{\max}(\lambda) \sim 0.2 \ln E_0 (\text{GeV}) + 0.7 \\ \sim 1 - 2 \lambda$$

- $10 - 11\lambda$ needed to contain showers upto $\sim 1\text{ TeV}$
- So, hadronic calorimeters must be much thicker than electromagnetic calorimeters.
- $\sim 95\%$ of shower laterally is contained in a cylinder of radius $\sim 1\lambda$.
 \Rightarrow Granularity need not be as fine as e.m. cell size \sim several cm.

A variety of processes involved in energy-loss.

\langle Fractional energy \rangle deposited by 10 GeV p in Fe/LAr
(Gabriel & Schmidt
ORNL TM-5105, 1975)

Process	% of total
Secondary proton ionization	31.6
Electromagnetic cascade (many π^\pm)	21.0 rises with E
Nuclear B.E. + γ production	20.6 invisible
Secondary π^\pm ionization	8.2
Neutrons $E > 10$ MeV	4.9
Neutrons $E < 10$ MeV	3.9
Residual nuclear excitation energy	3.7
$Z \geq 1$ particles ionization	2.3
Ionization by primary protons	1.4

Unlike e.m. showers which convert nearly all energy into ionization, hadronic showers produce a variable fraction of invisible energy.

- nuclear break-up absorbs binding energy
- neutrinos, low energy neutrons
- muons deposit very little energy

\Rightarrow much less signal than e.m. showers
"Compensation" needed

- Fluctuations between electromagnetic and hadronic components in a hadronic shower are large
 - Varying π^0 content → varying E.M. component
 - fluctuations in the nature of secondaries

⇒ worse energy resolution
- Even $\sim 10\lambda$ calorimeter may not contain a high energy hadronic shower ($> \sim 150$ GeV) completely (Containment issues)
 - "punchthrough" beyond the calorimeter or "leakage"
 - energy loss → degradation in energy resolution
(some correction can be applied)
 - background for other detectors beyond (mainly muon detectors)
- Hadronic showers are in general
 - longer
 - wider
 - fluctuate more
 - start later

than EM showers of same energy

COMPENSATION

In general,

Calorimeter response to hadrons < response to EM particles
at the same energy

$$\therefore \frac{e}{\pi} > 1$$

Also, calorimeter response to the EM component in hadronic showers is larger than to the hadronic component.

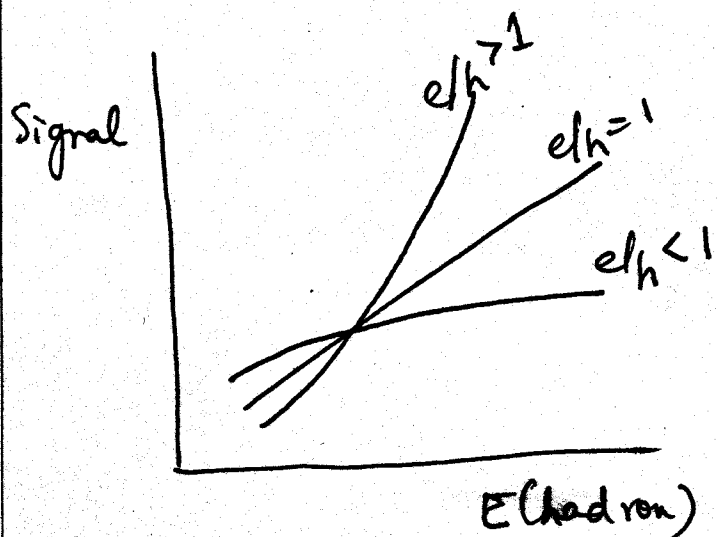
$$E_e/E_h > 1 \quad (\text{or } e/h > 1)$$

$$\text{Response } R_h = f_{EM} \cdot E_{EM} \cdot E_0 + (1 - f_{EM}) E_h E_0$$

$$R_e = E_{EM} \cdot E_0$$

$$\therefore \frac{e}{\pi} = \frac{R_e}{R_h} = \frac{E_{EM}}{E_h - f_{EM}(E_h - E_e)} = \frac{e/h}{1 - f_{EM}(1 - e/h)}$$

f_{EM} = fraction of EM energy within the hadronic shower
 $\approx 0.1 \ln(E(\text{GeV}))$



Energy Resolution:

$$\frac{\sigma(E)}{E} = \frac{a}{\sqrt{E}} + b \cdot \left| \frac{e}{h} - 1 \right|$$

Some examples:

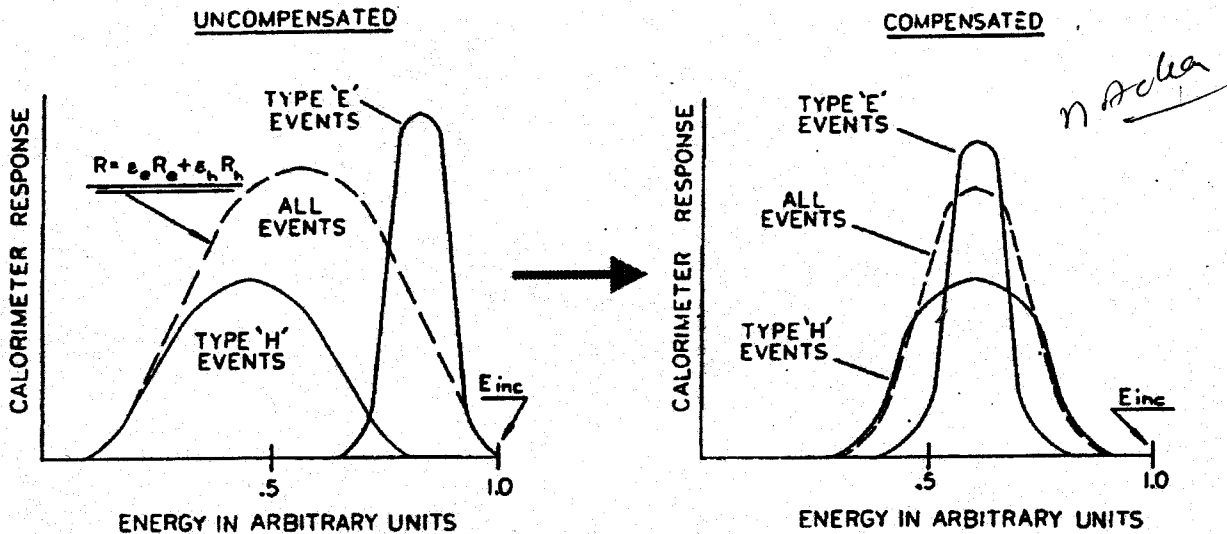
CDF Re/Sint $e/h \sim 1.6$

DΦ U/LAr $e/h \sim 1.1$
 ZEUS U/Scint $e/h \sim 1.0$

Need compensation $e/h \approx 1$; $e/\pi \approx 1$ for all E

Methods to Achieve compensation:

- increase E_h
 - use Uranium absorber \rightarrow amplify neutron and soft- γ component of fission
(extra energy released in ^{238}U fission compensates for the nuclear binding energy losses.)
 - use homogeneous active material \rightarrow high ϵ_h detection efficiency
- decrease E_e :
 - use thin sheets of passive low-Z material shielding the active medium
For $E < 1\text{ MeV}$, photoelectric effect is the important energy loss mechanism $\propto \text{photo} \propto Z^5$.
 \therefore Suppress low energy γ -detection.
 - off-line compensation possible but cumbersome.



(Cushman, Instrumentation In High Energy Physics, World Scientific, 1992)

Other Issues :

Longitudinal Leakage:

Finite size of the calorimeter

⇒ longitudinal & lateral leakage

Energy resolution gets degraded

$$\frac{\sigma(E)}{E} = \frac{\sigma(E)}{E} \left| (1 + f(E) + 50 \cdot f^2(E)) \right| \quad \frac{\sigma(E)}{E} \%$$

0%

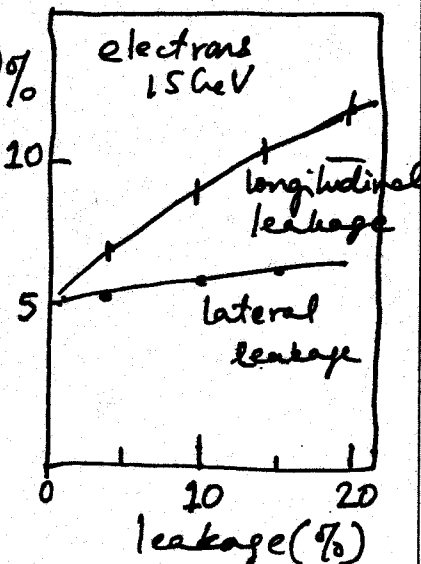
where,

$f(E)$ = lost energy fraction

(depends on energy)

Can install low-resolution

tail-catcher behind the hadronic
calorimeter.



Upstream Energy Loss:

- Showers start in "dead" material in front of calorimeter (other detectors, solenoid, support structures)
- Use Pre-shower detector in front of Calorimeter
 - recover some energy
 - improved background rejection due to better spatial resolution

— *Harmatic-dy*

Homogeneous Calorimeters

(2-5%)

- Excellent energy resolution since most of the energy is deposited in the active medium
- More difficult to segment laterally and longitudinally
- Mainly used as EM calorimeters in HEP.

- Scintillator calorimeters (crystals)
ionization \rightarrow light

BGO (Bismuth Germanate or $\text{Bi}_4\text{Ge}_3\text{O}_{12}$) used by L3
CsI (Tl) used by Babar
E735@CERN used NaI (Tl)

PbWO_4 (Lead Tungstate; to be used by ATLAS)

- Cerenkov Calorimeters

Material with high refractive index where relativistic e^\pm tracks in the shower produce Cerenkov photons.

E.g., PbO (Lead-Glass)

- Noble Liquid Calorimeters (Ar, Kr,..)

Noble gas at Cryogenic temperatures
ionization collected (LKr in NA48)

D/P

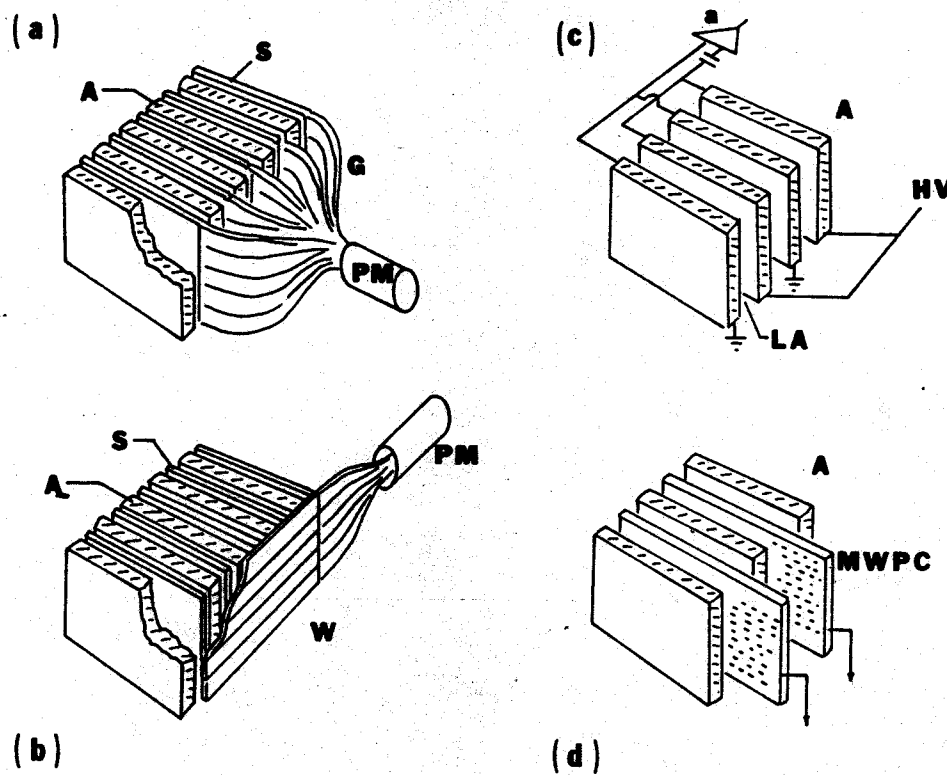
- Semiconductor Calorimeters (Si, Ge)

best energy resolution, but too compact for HEP.

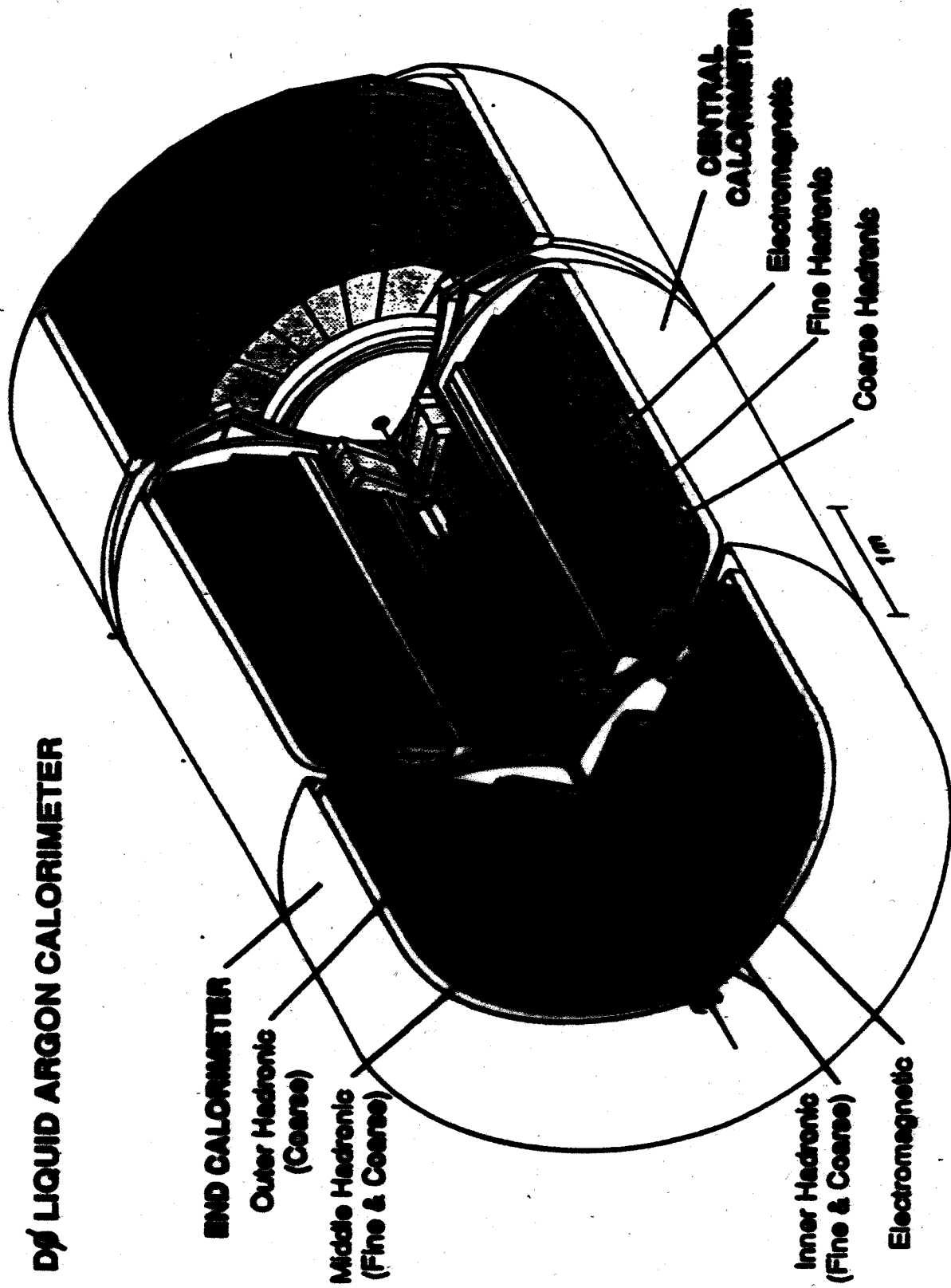
SAMPLING CALORIMETERS

- Absorber + detector (gaseous, liquid, solid) alternate
- MWPC, Streamer tubes
- Warm liquids (T_MP: Tetramethylpentane)
- Cryogenic noble liquids : LAr, LXe, LKr
- Scintillators, Scintillation fibers, Silicon detectors

Figure 11.4 Typical readout techniques for calorimeters: (a) lead-scintillator sandwich, (b) lead-scintillator sandwich with wavelength shifter bars, (c) liquid argon ionization chamber, and (d) lead-MWPC sandwich. (C. Fabjan and T. Ludlam, adapted with permission from the Annual Review of Nuclear and Particle Science, Vol. 32, © 1982 by Annual Reviews, Inc.)



D_Ø LIQUID ARGON CALORIMETER



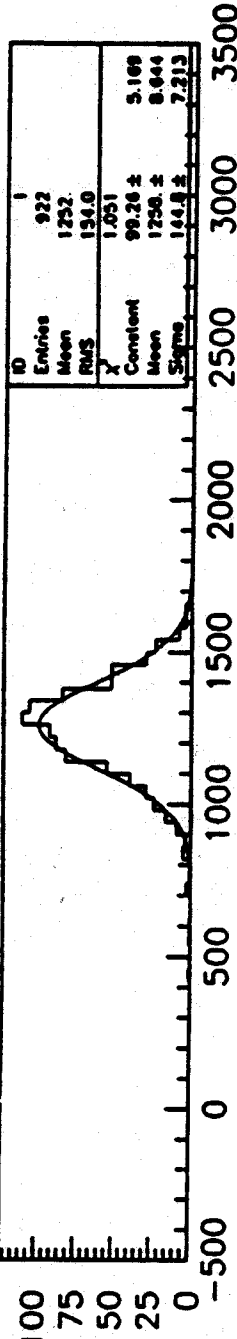
CC EM : 3 mm depleted U

EC EM : 4 mm

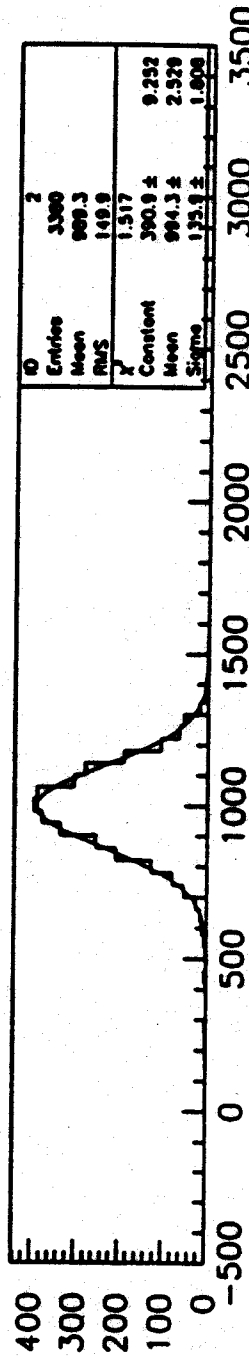
FH : 6 mm U-Nb (2%)

CCCH : 46.5 mm Cu ; ECCH : 46.5 mm

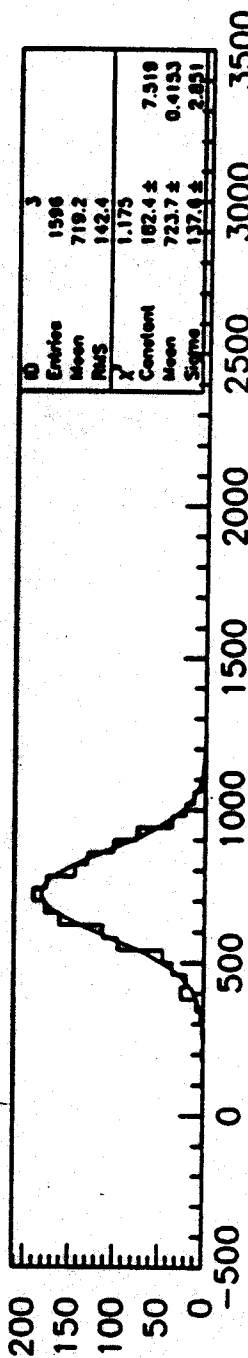
Test Beam Electrons eta=0.05, phi=31.6



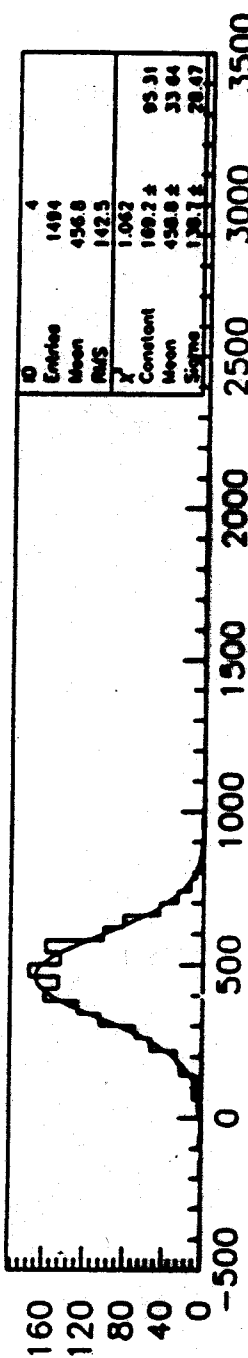
EMzTOT+FH1, 5 GeV



EMzTOT+FH1, 4 GeV



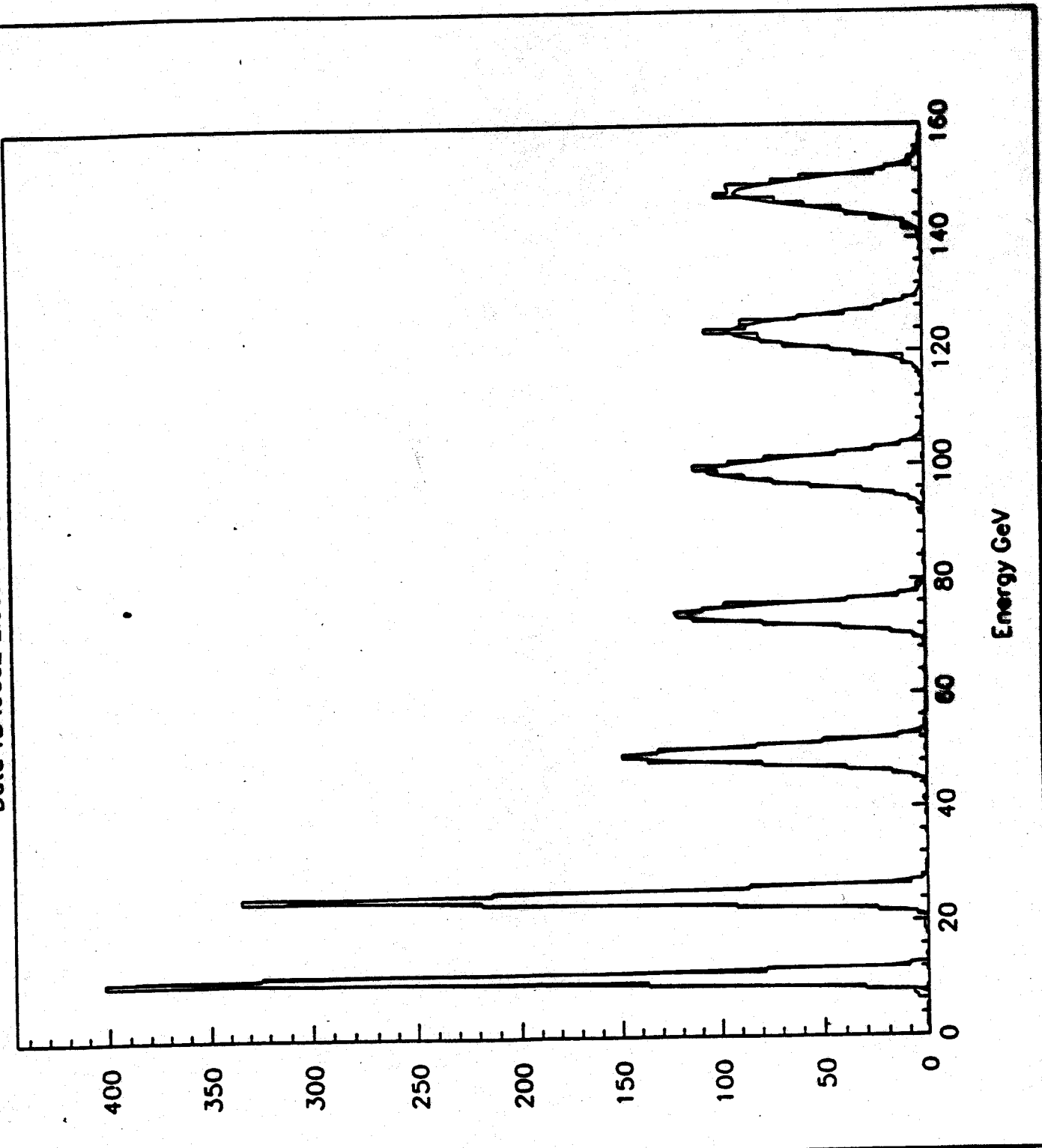
EMzTOT+FH1, 3 GeV



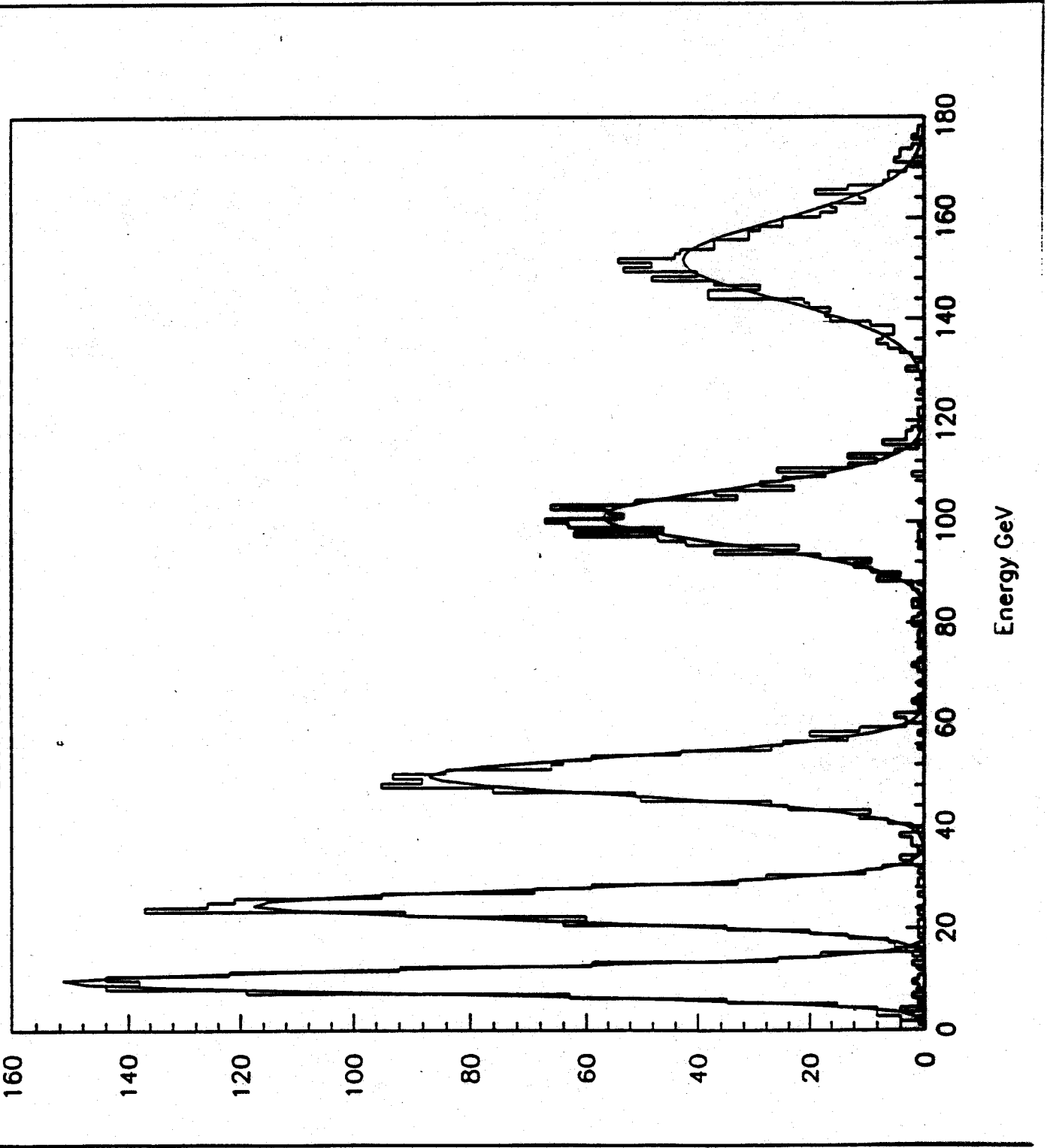
EMzTOT+FH1, 2 GeV

P. Bhaw (DP) DRF 1.7

Data TB load2 Electrons 0 to 150 GeV

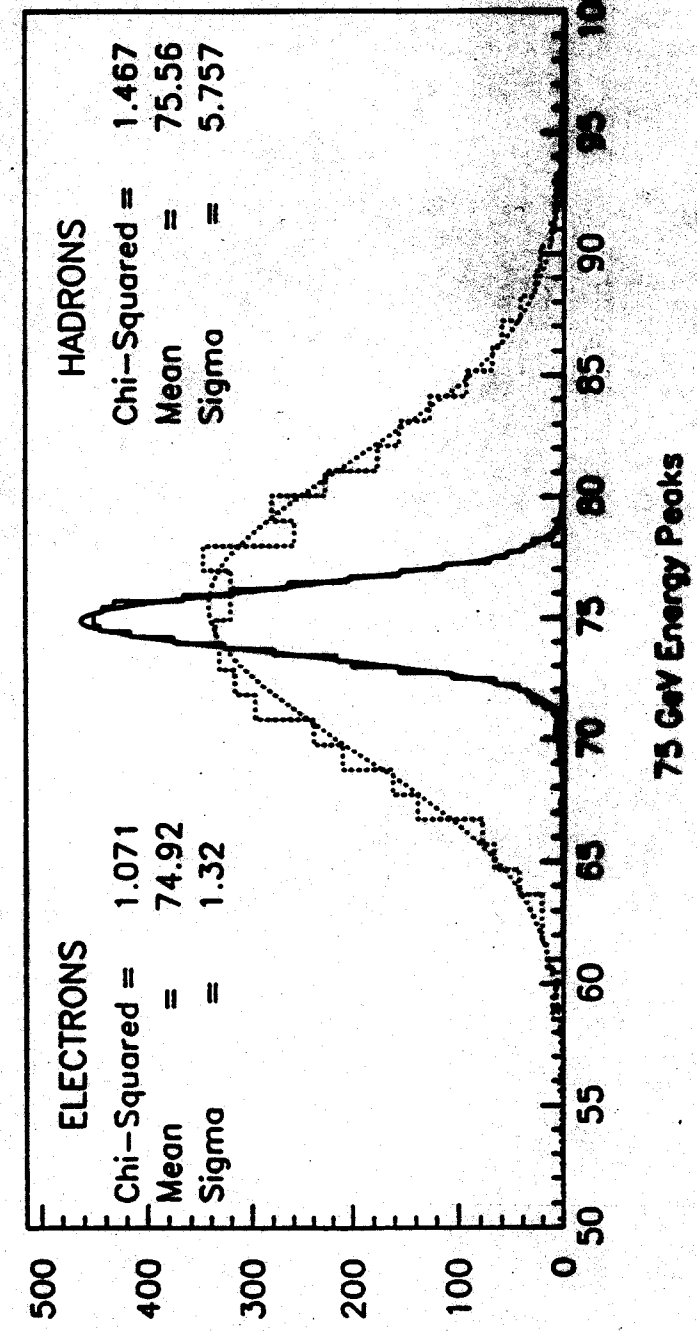
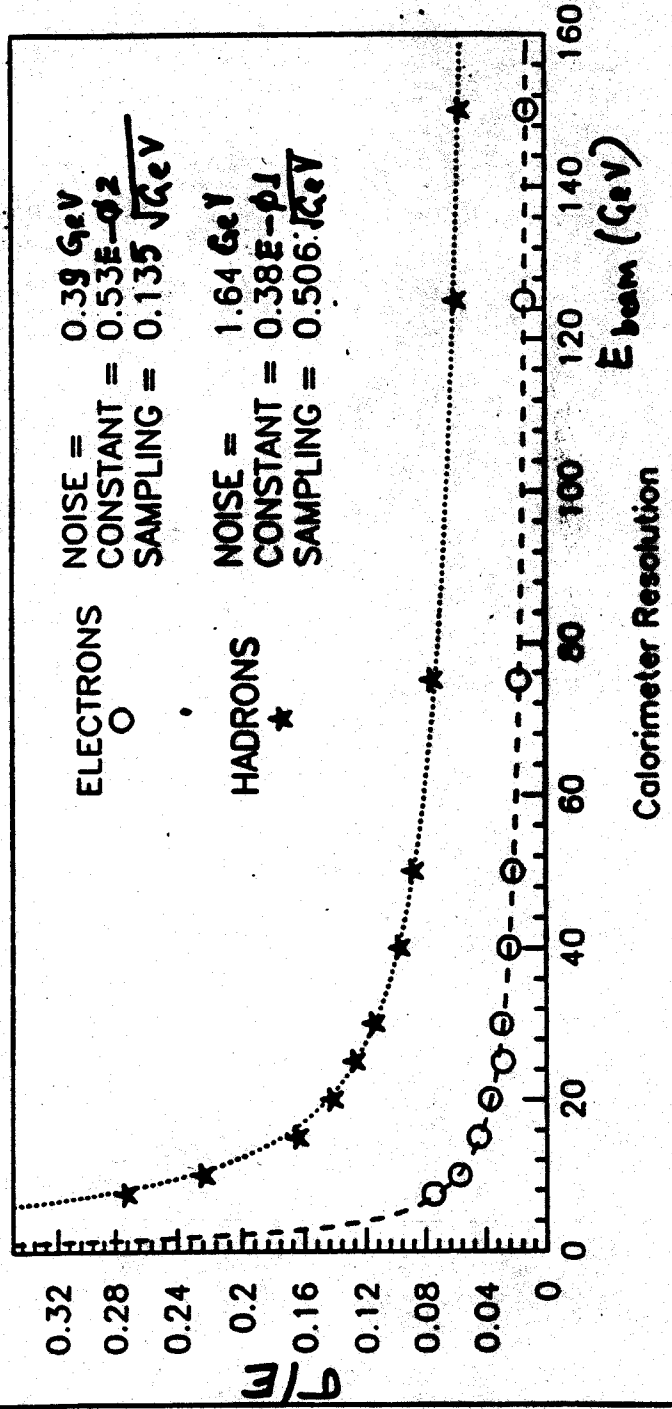


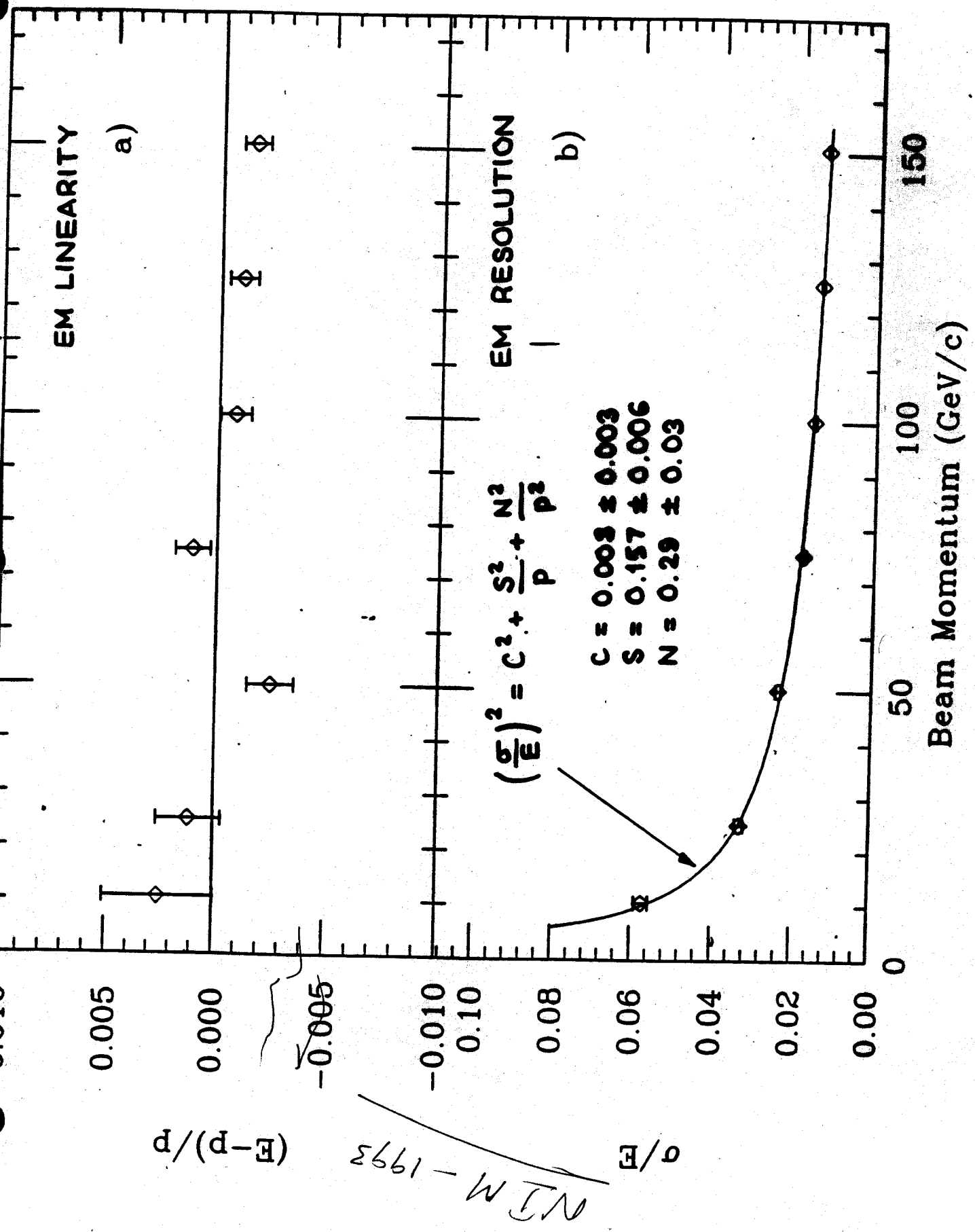
Data Test Beam Pions 10 to 150 GeV



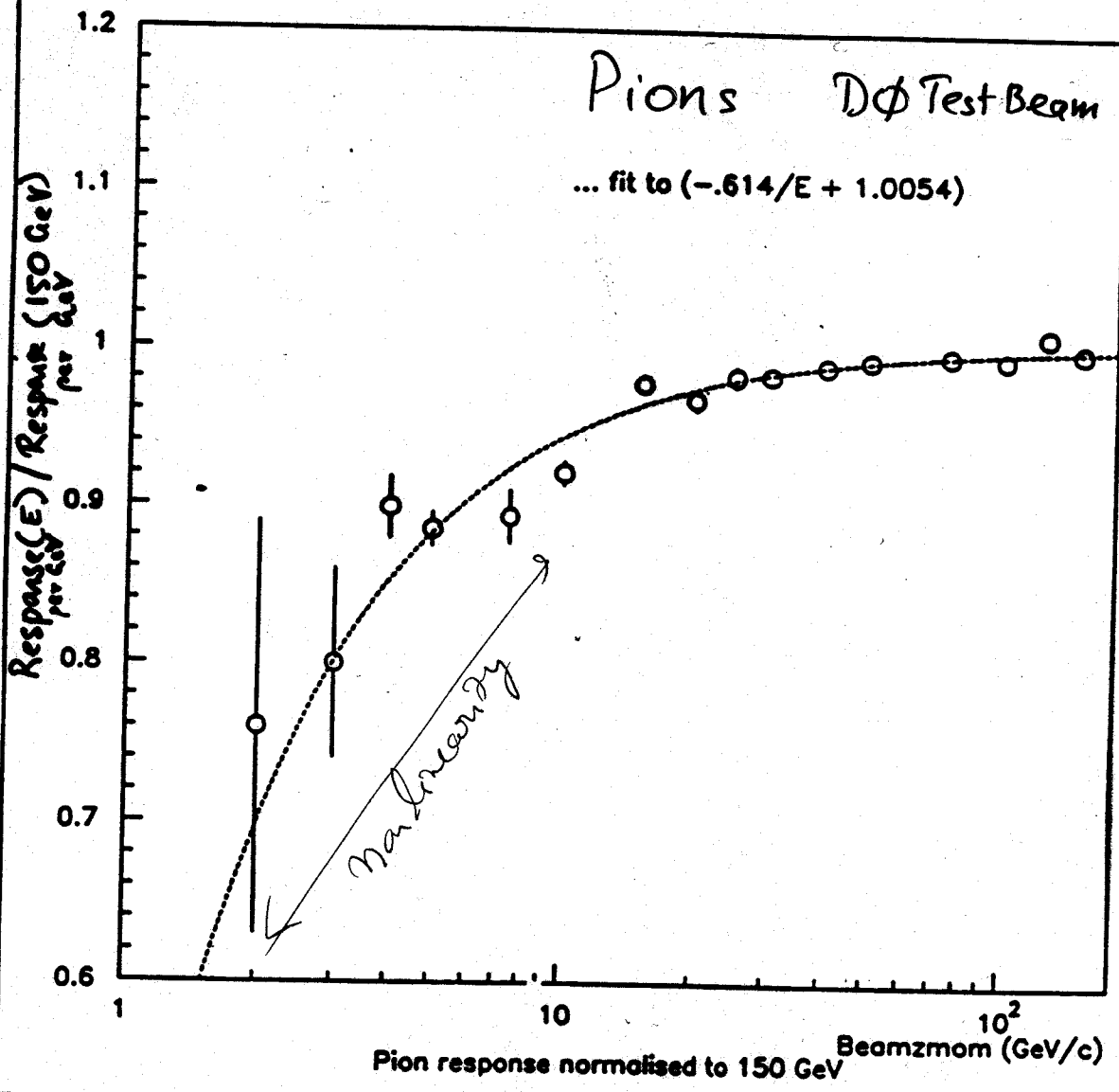
$$\left(\frac{dN}{dE}\right) = C - \frac{2}{E} + \frac{1}{E^2}$$

HIGH ENERGY RESULTS FOR ELECTRONS AND HADRONS





P.Bhat (D ϕ) DPF 1992



Experiment	Type	Resolution $\Delta E/E$	Reference
<i>Electromagnetic</i>			
Crystal Ball	NaI (TI)	$0.026/\sqrt{E}$	Bloom and Peck 1983
OPAL	Lead glass	$0.05/\sqrt{E}$	Akrawy <i>et al.</i> 1990
Crystal Barrel	CsI (TI)	$0.025/\sqrt{E}$	Landua 1996b
ZEUS	sampling: U + plastic scint.	$0.18/\sqrt{E}$	Behrens <i>et al.</i> 1990
D0	sampling: U + liquid Ar	$0.15/\sqrt{E}$	Abachi <i>et al.</i> 1994
ATLAS	sampling: Pb + liquid Ar	$0.10/\sqrt{E}$	Gingrich <i>et al.</i> 1995
<i>Hadronic</i>			
CHARM	sampling: Marble + scint.	$0.53/\sqrt{E}$	Diddens <i>et al.</i> 1980
ZEUS	sampling: U + plastic scint.	$0.35/\sqrt{E}$	Behrens <i>et al.</i> 1990
D0	sampling: U/Fe + liquid Ar	$0.50/\sqrt{E}$	Abachi <i>et al.</i> 1994

Note: All energies are to be taken in GeV; the constant terms, to be added quadratically, typically are a fraction of a percent for electromagnetic, and 0.02–0.03 for hadronic calorimeters.

increasing E , owing to the increasing number of neutrinos produced in